

Induced Eye-detectable Blue Emission of Triazolyl Derivatives *via* Selective Photodecomposition of Chloroform under UV Irradiation at 365 nm

Byoung-Kwan Lee, Jun Hee Yoon, Sangwoon Yoon, and Byoung-Ki Cho*

Department of Chemistry and Institute of Nanosensor and Biotechnology, Dankook University, Gyeonggi-Do 448-701, Korea

*E-mail: chobk@dankook.ac.kr

Received October 1, 2013, Accepted October 15, 2013

A bent-shape triazolyl derivative was synthesized *via* click chemistry, and its photophysical property was investigated in various solvents. In contrast to the invisible ultraviolet emission of other solutions, the chloroform solution exhibited a blue light emission at 460 nm. Furthermore, the blue fluorescence intensified as the UV exposure time at 365 nm increased. On the basis of $^1\text{H-NMR}$, pH paper, and acid-addition studies, we confirmed that chloroform was decomposed into HCl with the aid of the triazolyl derivative. The density functional theory calculations suggested that the eye-detectable blue fluorescence was attributed to an intramolecular charge transfer process of the protonated triazolyl derivative in the chloroform solution.

Key Words : Fluorescence, Chloroform photolysis, Click chemistry, Intramolecular charge transfer, Protonation

Introduction

Chloroform is one of the most common solvents because of its excellent solvation capability. It is directly degraded by UV irradiation at 184.9 nm because the UV source is sufficiently energetic to break the carbon-chlorine bond.¹ However, lower-energy lights with wavelengths longer than 253.7 nm cannot achieve photolysis of chloroform. Thus, inorganic photocatalysts, such as titanium oxide (TiO_2), are generally employed to decompose chloroform under lower-energy light sources.² In comparison to inorganic materials, chloroform decomposition of organic compounds has rarely been studied, although a porphyrin example was recently reported.³

“Turn-on” fluorescence under a certain condition is an interesting phenomenon, and thereby this has been extensively studied in sensing a specific target.⁴ Due to its rapid response, excellent sensitivity and bio-imaging application, the “turn-on” approach is more desirable than the opposite “turn-off” way. In addition to a target-sensing, this approach can also be employed as an indicator for a certain reaction.⁵ In particular, a visible-range emission induced by chemical reactions is advantageous because of its detectability with the naked eye.

Herein, we present a “turn-on” fluorescence phenomenon

induced by a selective photo-degradation of chloroform. In this work, we employed a bent triazolyl derivative **1** as the photocatalyst, which can decompose chloroform under UV irradiation at 365 nm (Figure 1(a)). Considering the inertness of chloroform under the 365 nm-UV, the chloroform decomposition in the presence of **1** is a very unique phenomenon. In addition, strong blue fluorescence was induced only in the chloroform solution and not in other solutions (Figure 1(b)). The selective occurrence of eye-detectable fluorescence induction in the chloroform solution points to the triazolyl derivative having photosensitizing capability.

Experimental

General Methods. ^1H -, and ^{13}C -NMR spectra were recorded from a CDCl_3 solution using Varian 200 and Bruker AM 500 spectrometers. The purity of the products was checked by thin-layer chromatography (TLC; Merck, silica gel 60). Gel permeation chromatography (GPC) measurements were conducted in THF and *N,N'*-dimethylacetamide (99.9%) (98:2 volume ratio) using a Waters 401 instrument equipped with Stragel HR 2,3 columns and Shodex AT-8045 at a flow rate of 1.0 mL/min. Absorption spectra were obtained on a Perkin Elmer spectrum Lambda 950 UV/Vis/NIR spectrophotometer. Fluorescence spectra were recorded with a Hitachi F-7000 fluorescence spectrophotometer. Element analyses were performed with a Perkin Elmer 240 elemental analyzer at the Organic Chemistry Research Center, Sogang University, Korea. MALDI TOF-mass spectra were obtained on a Voyager-DETM STR Biospectrometry Workstation at the National Center for Inter-University Research Facilities, Seoul National University (SNU). The UV hand lamp used in this study was Spectroline ENF-240C/FE (6 W, 254 nm/365 nm). Dynamic light scattering (DLS) measurements were performed using a zeta-potential and particle-size analyzer ELSZ-2 (Photal, Japan).

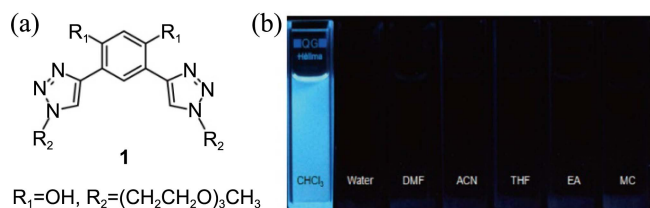
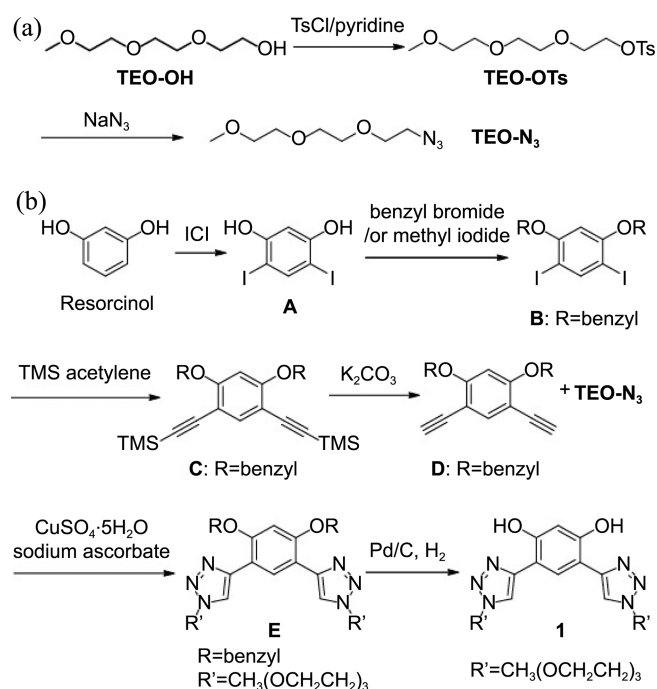


Figure 1. (a) Molecular structure of triazolyl derivative **1** and (b) the eye-detectable blue-light emission exclusively in the chloroform solution of **1**. DMF, ACN, THF, EA and MC indicate *N,N'*-dimethylformamide, acetonitrile, tetrahydrofuran, ethyl acetate, and dichloromethane, respectively.



Scheme 1. Synthetic routes of (a) azide-functionalized tri(ethylene oxide) coil and (b) triazolyl derivative **1**.

Synthesis. The general synthetic procedure is outlined in Schemes 1.

Synthesis of TEO-OTs. TEO-OH (5.0 g, 30.4 mmol), 4-toluenesulfonyl chloride (17.42 g, 91.0 mmol) and pyridine (7.34 mL, 91.0 mmol) were dissolved in 100 mL of dichloromethane. The reaction mixture was stirred for 1 day at room temperature under an N₂ atmosphere. The reaction mixture was extracted with dichloromethane and diluted HCl solution three times, and dried over anhydrous MgSO₄. After removing dichloromethane in a rotary evaporator, the resulting compound was purified by a silica gel column chromatography using dichloromethane:ethyl acetate = 1:1 as the eluent, to yield 8.39 g (86.5%) of a colorless liquid. ¹H-NMR (CDCl₃) δ 7.78 (d, 2H, *J* = 8.2 Hz, Ar-H), 7.36 (d, 2H, *J* = 8.0 Hz, Ar-H), 4.16 (t, *J* = 4.8 Hz, 2H, -OCH₂), 3.68–3.54 (m, 10H, CH₂(OCH₂CH₂)₂), 3.37 (s, 3H, -OCH₃), 2.45 (s, 3H, Ar-CH₃).

Synthesis of TEO-N₃. TEO-OTs (8.39 g, 26.4 mmol) and sodium azide (5.13 g, 79 mmol) were dissolved in 30 mL of dry DMF. The reaction mixture was heated to reflux for 12 hours under an N₂ atmosphere. After cooling to room temperature, the solvent was removed by a rotary evaporator. The mixture was extracted with dichloromethane and deionized water one time, and dried over anhydrous MgSO₄. After removing dichloromethane in a rotary evaporator, the resulting compound was purified by a silica gel column chromatography to dichloromethane as eluent, to yield 4.53 g (90.9%) of a colorless liquid. ¹H-NMR (CDCl₃) δ 3.67–3.54 (m, 10H, CH₂(OCH₂CH₂)₂), 3.37 (s, 3H, -OCH₃), 3.35 (m, 2H, N₃-CH₂).

Synthesis of Compound A. To iodine monochloride (10.46 mL, 200 mmol) in 50 mL of dry ether, resorcinol (10

g, 90.6 mmol) in 100 mL of dry ether was added dropwise at 0 °C. The mixture was stirred at room temperature for 2 hours. After cooling to 0 °C, excess of Na₂S₂O₃ was added slowly and stirred for 30 min. The reaction mixture was extracted with diethyl ether and deionized water one time, and then dried over anhydrous MgSO₄. After removing diethyl ether in a rotary evaporator, the resulting compound was washed with deionized water. The resulting precipitate was extracted with ethyl acetate and deionized water once, and then dried over anhydrous MgSO₄. After removing ethyl acetate in a rotary evaporator, 23.8 g (72.4%) of a pale red solid was yielded. ¹H-NMR (CDCl₃) δ 7.84 (s, 1H, Ar-H), 6.71 (s, 1H, Ar-H), 5.24 (s, 2H, -OH).

Synthesis of Compound B. Compound A (11.5 g, 31.8 mmol), benzyl bromide (16.43 mL, 138.0 mmol) and potassium carbonate (19.1 g, 138.0 mmol) were dissolved in 100 mL of dry methyl ethyl ketone. The reaction mixture was heated to reflux for 12 h under N₂ atmosphere. The solvent was removed by a rotary evaporator. The resulting mixture was extracted with dichloromethane and deionized water three times, and then dried over anhydrous MgSO₄. After removing dichloromethane in a rotary evaporator, the resulting compound was purified by a silica gel column chromatography using *n*-hexane:dichloromethane = 4:1 as the eluent, to yield 12.47 g (72.3%) of a white solid. ¹H-NMR (CDCl₃) δ 8.09 (s, 1H, Ar-H), 7.42–7.36 (m, 10H, benzyl-H), 6.41 (s, 1H, Ar-H), 5.07 (s, 4H, CH₂).

Synthesis of Compound C. Compound B (6.0 g, 11.1 mmol), ethynyltrimethylsilane (6.3 mL, 44.3 mmol) and diisopropylamine (12.41 mL, 88.5 mmol) in 40 mL of dry THF were degassed. CuI (50 mg, 0.263 mmol) and PdCl₂(PPh₃)₂ (40 mg, 0.057 mmol) were added and heated to reflux for 4 h under N₂ atmosphere. After cooling to room temperature, THF was removed by a rotary evaporator. The reaction mixture was extracted with dichloromethane and deionized water three times, and then dried over anhydrous MgSO₄. After removing dichloromethane in a rotary evaporator, the resulting compound was purified by a silica gel column chromatography using *n*-hexane:dichloromethane = 15:1 as the eluent, to yield 3.79 g (71.2%) of a pale yellow solid. ¹H-NMR (CDCl₃) δ 7.60–7.31 (m, 12H, Ar-H), 6.43 (s, 1H, Ar-H), 5.12 (s, 4H, CH₂), 0.23 (s, 18H, Si-CH₃).

Synthesis of Compound D. Compound C (2.4 g, 4.9 mmol) and potassium carbonate (8.3 g, 59.7 mmol) were dissolved in 15 mL of THF and 15 mL of methanol. The reaction mixture was stirred for 3 hours under N₂ atmosphere. The solvent was removed by a rotary evaporator. The resulting mixture was extracted with dichloromethane and deionized water three times, and then dried over anhydrous MgSO₄. After removing dichloromethane in a rotary evaporator, the resulting compound was purified by a silica gel column chromatography using *n*-hexane:dichloromethane = 5:1 as the eluent, to yield 1.13 g (67.2%) of a white solid. ¹H-NMR (CDCl₃) δ 7.57 (s, 1H, Ar-H), 7.36–7.34 (m, 10H, benzyl-H), 6.42 (s, 1H, Ar-H), 5.10 (s, 4H, CH₂), 3.22 (s, 2H, Ar-C≡CH).

Synthesis of Compound E. Compound D (1.12 g, 3.3 mmol), TEO-N₃ (1.51 g, 8.0 mmol), sodium ascorbate (1.32

g, 6.7 mmol), and $\text{CuSO}_4 \cdot 5\text{H}_2\text{O}$ (0.83 g, 3.3 mmol) were dissolved in 15 mL of THF and 3 mL of deionized water. The reaction mixture was stirred for 12 h under N_2 atmosphere. The solvent was removed by a rotary evaporator. The resulting mixture was extracted with dichloromethane and deionized water three times, and then dried over anhydrous MgSO_4 . After removing dichloromethane in a rotary evaporator, the resulting compound was purified by a silica gel column chromatography using ethyl acetate as the eluent, to yield 1.97 g (82.3%) of a colorless liquid. $^1\text{H-NMR}$ (CDCl_3) δ 9.15 (s, 1H, Ar-H), 7.97 (s, 2H, triazole-H), 7.38 (s, 10H, benzyl-H), 6.65 (s, 1H, Ar-H), 5.13 (s, 4H, CH_2), 4.49 (t, $J = 5.1$ Hz, 4H, N- CH_2), 3.85 (t, $J = 5.1$ Hz, 4H, $-\text{OCH}_2$), 3.51–3.46 (m, 16H, $-(\text{OCH}_2\text{CH}_2)_2$), 3.30 (s, 6H, $-\text{OCH}_3$).

Synthesis of Triazolyl Derivative (1). To a solution of **E** (1.93 g, 2.7 mmol) in dry THF 20 mL was added 10 wt % Pd/C (56 M%), and the reaction solution was degassed for 5 times with H_2 gas. The reaction mixture was stirred at room temperature for 12 h in the presence of H_2 gas. Then, Pd catalyst was filtered off and the filtrate was concentrated under reduced pressure. The residue was purified by a silica gel column chromatography using ethyl acetate:methanol = 20:1 as the eluent, to yield 1.09 g (74.15%) of a pale yellow liquid. $^1\text{H-NMR}$ (500 MHz, CDCl_3) δ 10.93 (s, 2H, $-\text{OH}$), 8.05 (s, 2H, triazole-H), 7.60 (s, 1H, Ar-H), 6.70 (s, 1H, Ar-H), 4.61 (t, $J = 4.8$ Hz, 4H, $-\text{NCH}_2$), 3.95 (t, $J = 4.9$ Hz, 4H, $-\text{OCH}_2$), 3.64–3.50 (m, 16H, $-(\text{OCH}_2\text{CH}_2)_2$), 3.30 (s, 6H, $-\text{OCH}_3$). $^{13}\text{C-NMR}$ (125 MHz, CDCl_3) δ 157.63, 147.46, 123.80, 119.78, 107.55, 105.48, 77.52, 77.26, 77.01, 72.08, 70.79, 70.69, 69.57, 59.17, 50.98. M_w/M_n (GPC) = 1.01. Anal. Calcd for $\text{C}_{24}\text{H}_{36}\text{N}_6\text{O}_8$: C, 53.72; H, 6.76; N, 15.66. Found: C, 53.73; H, 6.47; N, 15.24. MALDI-TOF MS: 537.46 $[\text{1}+\text{H}]^+$, 559.46 $[\text{1}+\text{Na}]^+$.

Results and Discussion

For the synthesis, an efficient click reaction was employed to prepare the triazolyl derivative (**1**).⁶ The synthetic procedure is briefly described below. The azido compound was prepared by sequential tosylation and azidation reaction of tri(ethylene glycol) monomethyl ether (Scheme 1(a)). 4,6-Diethynyl benzene was synthesized through iodination of resorcinol, hydroxyl group protection, Sonogashira coupling, and deprotection of trimethylsilyl group. The click coupling of the prepared azide and alkynyl precursors yielded a benzylated intermediate, which could be converted into the final triazolyl compound by a debenzylation reaction (Scheme 1(b)).

The triazolyl derivative was characterized by $^1\text{H-NMR}$, $^{13}\text{C-NMR}$, gel permeation chromatography (GPC), matrix-assisted laser desorption/ionization time-of-flight mass spectrometry (MALDI-TOF MS), and elemental analysis. In the $^1\text{H-NMR}$ spectrum, the triazolyl hydrogen and the hydroxyl proton appeared at 7.8 ppm and 10.9 ppm, respectively, and the $^{13}\text{C-NMR}$ spectrum showed six distinct aromatic carbons (Figure S1). Additionally, the molecular mass from the MALDI-TOF MS was consistent with the theoretical mass,

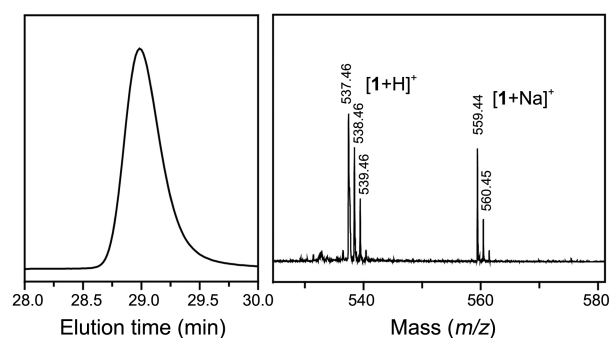


Figure 2. GPC and MALDI-TOF MS data of **1**.

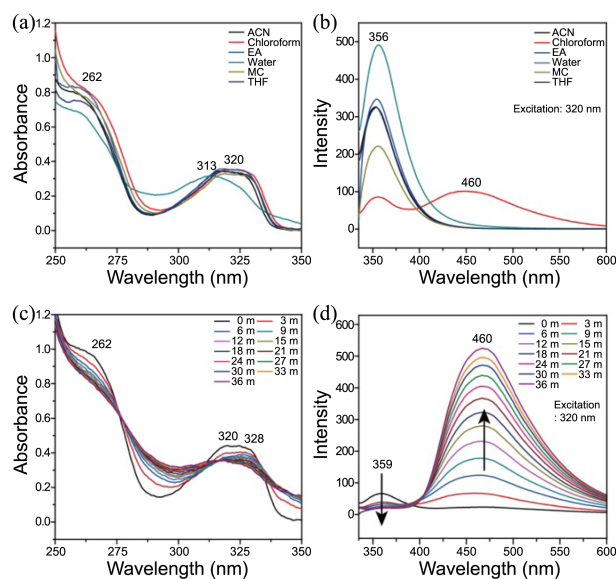


Figure 3. (a) Absorption and (b) emission spectra of **1** in various solvents. (c) Absorption and (d) emission spectra of the chloroform solution as a function of the exposure time to UV radiation at 365 nm.

and the molecular weight distribution from the GPC was narrow, indicative of high purity (Figure 2).

The photophysical properties of the triazolyl derivative were analyzed in various solvents. In most solutions, the absorption maxima were revealed at 262 nm and 320 nm (Figure 3(a)). The aqueous solution exhibited a slight hypsochromic shift because of the interruption of the intramolecular hydrogen bonding between the hydroxyl and nitrogen groups.⁷ On the basis of the absorption spectra, we investigated the fluorescence properties with the excitation at 320 nm (Figure 3(b)). Most of the solutions exhibited an emission band with $\lambda_{\text{max}} = 356$ nm, while only the chloroform solution showed additional bathochromic emission with $\lambda_{\text{max}} = 460$ nm along with the emission at 356 nm. In contrast to the invisible UV emission at 356 nm, the emission at 460 nm corresponds to the blue-light region. Therefore, the chloroform solution could be distinguishable from other solutions with the naked eye.

Moreover, the optical properties of the chloroform solution were investigated as a function of the exposure time to a 365 nm UV hand lamp. As the exposure time increased, the

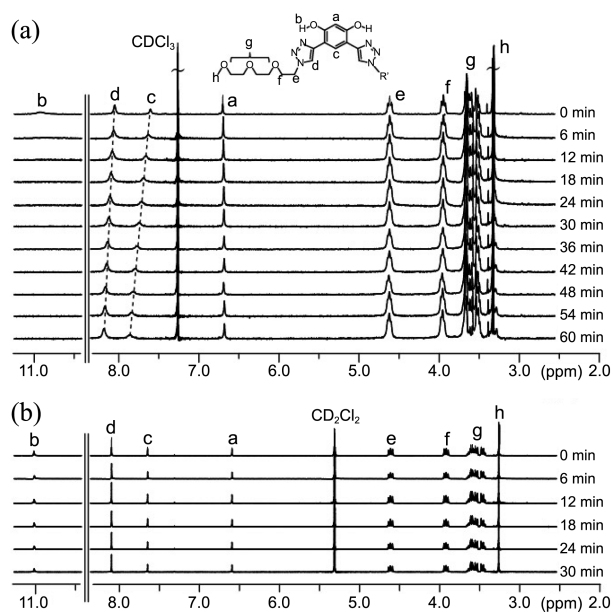


Figure 4. $^1\text{H-NMR}$ spectra of **1** in (a) chloroform (b) dichloromethane as a function of the 365 nm-UV irradiation time.

260 nm and 320 nm absorption bands were red-shifted, and finally the spectrum became broader (Figure 3(c)). In the fluorescence, as expected, the chloroform solution displayed a blue emission that was detectable with the naked eye (Figure 1(b)). Remarkably, the blue emission became intensified as the irradiation time increased, whereas the emission at 360 nm grew weaker (Figure 3(d)).

To understand the reason for the unique fluorescence behavior of the chloroform solution, we first suspected the formation of aggregates, which could induce bathochromic emission in many cases.⁸ This was investigated using a dynamic light scattering (DLS) technique. No aggregation was observed because the autocorrelation function did not fall in the DLS data (Figure S2). Thus, this possibility was ruled out.

We then speculated that a photochemical reaction occurred in the chloroform solution under the UV irradiation at 365 nm.⁹ The $^1\text{H-NMR}$ spectra of the chloroform solution were examined as the UV exposure time increased (Figure 4(a)). The benzenyl proton *meta* to the hydroxyl group and the triazolyl proton moved downfield, and the hydroxyl group at 10.9 ppm disappeared. Along with the $^1\text{H-NMR}$ results, the UV absorption spectral variation may also be an indication of the occurrence of structural variation during the UV irradiation (Figure 3(c)). Such spectroscopic changes must be mediated by a change in the chloroform molecule instead of a direct structural change in the triazolyl derivative. This could be demonstrated by a comparative study with the dichloromethane solution of **1**. In contrast to the chloroform solution, no $^1\text{H-NMR}$ spectral change was found in the dichloromethane (Figure 4(b)). The results suggest the following probable scenario: the chemical reaction of chloroform during the 365 nm-UV irradiation yields a photochemical product, which subsequently influences the structure of the triazolyl derivative, resulting in the eye-detectable blue-light

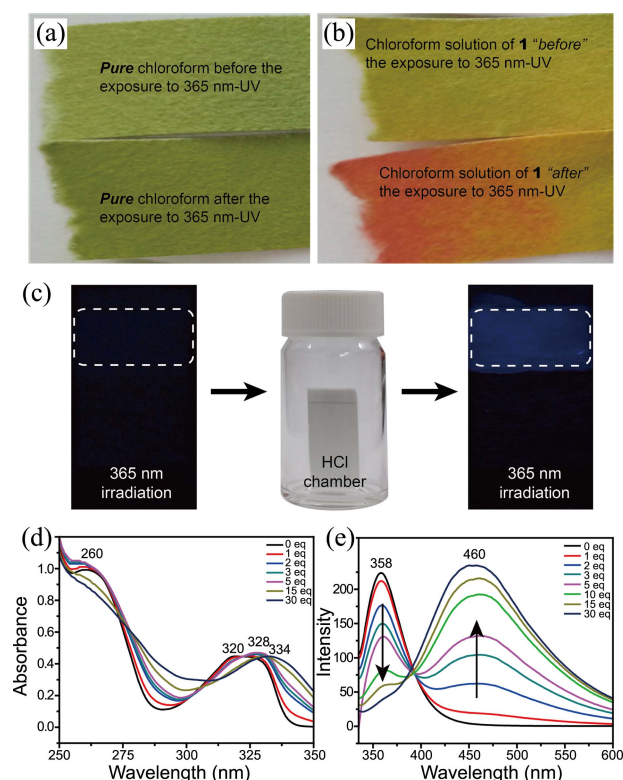


Figure 5. pH papers of (a) pure chloroform and (b) the chloroform solution of **1** before and after the exposure to 365 nm-UV light. The exposure time was 1 h. (c) Induced blue-light emission of triazolyl derivative **1** on the TLC plate after placement in a saturated HCl chamber. (d) Absorption and (e) emission spectral variations of the dichloromethane solution of **1** upon the addition of HCl.

emission.

Chloroform is known to be decomposed into HCl under UV irradiation at “185 nm” but intact UV radiation at “365 nm”.¹ Indeed, we did not observe acid generation from pure chloroform with the 365 nm UV lamp. No color change in a pH paper was found (Figure 5(a)). Therefore, the triazolyl derivative was involved in the photolysis of chloroform. An identical experiment was carried out in the presence of the triazolyl derivative (**1**). As shown in Figure 5(b), the pH paper became reddish, indicating acid generation. Consequently, the presence of the triazolyl derivative played a critical role in the photodegradation of chloroform.

In addition to the chloroform degradation, another interesting aspect in this study was the induction of the blue-light fluorescence in response to the generation of acid. To explain this, we examined the fluorescence change of **1** in a saturated HCl chamber. After exposure to the HCl gas for about 5 min, the sample region on the TLC plate displayed blue-light emission under the UV light at 365 nm, which is consistent with the fluorescence behavior of the chloroform solution (Figure 5(c)). Therefore, it can be said that the blue-light emission induction was mainly attributed to the interaction between the triazolyl derivative and HCl, because chloroform was not used in this test. This was further confirmed by investigating the absorption and emission spectra

of the dichloromethane solution in response to the addition of methanolic HCl, because the dichloromethane solution is stable at the excitation with 320 nm.¹⁰ As the HCl concentration increased, the absorption spectrum red-shifted, suggestive of charge transfer character (Figure 5(d)).¹¹ In the emission spectra, the blue emission with $\lambda_{\text{max}} = 460$ nm was intensified, whereas the initially intense emission at 360 nm was diminished (Figure 5(e)). These photophysical properties were identical to those of the chloroform solution of **1**. Consequently, these investigations indicate that the triazolyl derivative assists the photo-decomposition of chloroform into HCl under the UV irradiation at 365 nm, which subsequently influences the electronic structure of the triazolyl derivative.

Considering the molecular structure, the non-bonding electrons of the triazolyl rings must be protonated by HCl. The stoichiometry of the protonation of the triazole derivative was analyzed using the Bensei-Hildebrand (B-H) method. The data in Figure 5(e) were used for the calculation. As the two nitrogen atoms of each triazole ring in **1** could be protonated, we investigated four protonation cases. The best fit was observed in the protonation stoichiometry of 2, indicating that a nitrogen atom in each triazole was protonated by HCl (Figure S3).¹² To evaluate the electron density in each nitrogen atom, we performed density functional theory (DFT) calculations. According to the electron density map of **1**, the middle nitrogen atom of the triazole ring was the most electron-rich (Figure S4). Therefore, the protonation may occur there.

Upon protonation of the triazole ring, the fluorescence spectrum red-shifted from the UV to the visible region. The magnitude of this shift was as large as 100 nm. Similar emission properties have been found in several conjugated heterocyclic compounds that closely resemble our triazolyl

compound in appearance.¹³ In these compounds, the protonation of aromatic heterocyclic nitrogen caused an electron transfer from neighboring electron-rich groups to the protonated heterocycles. This intramolecular charge transfer formed a more stable excited state. Therefore, the energy gap between the highest occupied and the lowest unoccupied molecular orbitals (HOMO and LUMO) became reduced, resulting in red-shifted fluorescence phenomena. Our observation (*i.e.*, the bathochromic emission shift by 100 nm upon protonation) could be explained in terms of this charge transfer process. In comparison to unprotonated **1**, the triazole rings of protonated **1** become more electropositive. Therefore, when the molecule was excited, the electron transfer to the protonated triazole was promoted *via* the formation of a stable charge transfer state.

To support the argument for the intramolecular charge transfer, we calculated frontier molecular orbitals of the unprotonated and protonated models using the DFT (B3LYP/6-31+G(d,p)). In the unprotonated model, the HOMO and LUMO were distributed over the benzenyl and the triazolyl rings (Figure 6(a)). In the protonated model, on the other hand, the electrons delocalized over the aromatic rings in HOMO became localized on the protonated triazolyl rings in LUMO (Figure 6(b)). Furthermore, the HOMO-LUMO energy gap red-shifted upon protonation (from 4.33 eV to 3.40 eV). These DFT calculations are consistent with the observed photophysical properties, suggesting that the intramolecular charge transfer is highly likely to be the mechanism underlying the red-shifted emission of the protonated triazolyl derivatives.¹⁴ In contrast to the invisible UV emitted solitons, the acid-generating chloroform solution emitted the eye-detectable blue-light due to the formation of the charge transfer state of the protonated molecule.

Conclusion

A bent-shaped triazole derivative was prepared by a click reaction, and its photophysical property was investigated in various solvents. Most of solution samples exhibited fluorescence in the UV region, but only the chloroform solution displayed eye-detectable blue-light emission. The ¹H-NMR, pH paper, and comparative acid-addition experiments indicated that the chloroform molecules were abnormally decomposed into HCl by UV radiation at 365 nm, which was assisted by the triazole derivative. The induced blue-light emission of the chloroform solution involved the protonation of the triazolyl group. It could be interpreted in terms of intramolecular charge transfer from the electron-rich central benzenyl group to the electropositive protonated triazoles.

Acknowledgments. The present research was conducted by the research fund of Dankook university in 2013.

Supporting Information. The supporting Information is available on request from the corresponding author (E-mail: chobk@dankook.ac.kr).

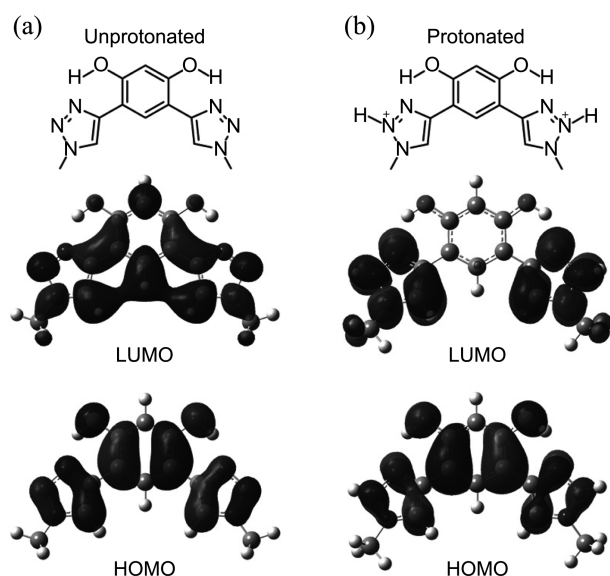


Figure 6. Frontier orbitals (HOMO and LUMO) of (a) unprotonated and (b) protonated models. For the DFT calculation, the molecular model has methyl groups instead of tri(ethylene glycol) chains.

References

1. (a) Alapi, T.; Dombi, A. *Chemosphere* **2007**, *67*, 693. (b) Kuwahara, Y.; Zhang, A.; Soma, H.; Tsuda, A. *Org. Lett.* **2012**, *14*, 3376.
 2. (a) Kang, M.; Lee, S.-Y.; Chung, C.-H.; Cho, S. M.; Han, G. Y.; Kim, B.-W.; Yoon, K. J. *J. Photochem. Photobiol. A: Chem.* **2001**, *144*, 185. (b) Peña, L. A.; Seidl, A. J.; Cohen, L. R.; Hoggard, P. E. *Transition Met. Chem.* **2009**, *34*, 135.
 3. Muñoz, Z.; Cohen, A. S.; Nguyen, L. M.; McIntosh, T. A.; Hoggard, P. E. *Photochem. Photobiol. Sci.* **2008**, *7*, 337.
 4. Nolan, E. M.; Lippard, S. J. *J. Am. Chem. Soc.* **2003**, *125*, 14270.
 5. Yu, Z.; Ho, L. Y.; Lin, Q. *J. Am. Chem. Soc.* **2011**, *133*, 11912.
 6. (a) Ryu, M.-H.; Choi, J.-W.; Kim, H.-J.; Park, N.; Cho, B.-K. *Angew. Chem. Int. Ed.* **2011**, *50*, 5737. (b) Lee, S.; Hua, Y.; Park, H.; Flood, A. H. *Org. Lett.* **2010**, *12*, 2100. (c) Cao, Q.-Y.; Pradhan, T.; Lee, M. H.; No, K.; Kim, J. S. *Analyst* **2012**, *137*, 4454.
 7. Helal, A.; Lee, S. H.; Ren, W. X.; Cho, C. S.; Kim, H.-S. *Bull. Korean Chem. Soc.* **2011**, *32*, 1599.
 8. (a) Kumbhakar, M. *J. Phys. Chem. B* **2007**, *111*, 14250. (b) Pierola, I. F.; Agzenai, Y. *J. Phys. Chem. B* **2012**, *116*, 3973. (c) Wu, J.; Liu, W.; Ge, J.; Zhang, H.; Wang, P. *Chem. Soc. Rev.* **2011**, *40*, 3483.
 9. Giordani, S.; Cejas, M. A.; Raymo, F. M. *Tetrahedron* **2004**, *60*, 10973.
 10. Mhuircheartaigh, É. M. N.; Blau, W. J.; Prato, M.; Giordani, S. *Carbon* **2007**, *45*, 2665.
 11. (a) Liu, Y.; Yu, Y.; Gao, J.; Wang, Z.; Zhang, X. *Angew. Chem. Int. Ed.* **2010**, *49*, 6576. (b) Liu, K.; Wang, C.; Li, Z.; Zhang, X. *Angew. Chem. Int. Ed.* **2011**, *50*, 4952. (c) Jana, P.; Maity, S.; Maity, S. K.; Ghorai, P. K.; Haldar, D. *Soft Matter* **2012**, *8*, 5621.
 12. (a) Huo, D.; Yang, L.; Hou, C.; Fa, H.; Luo, X.; Lu, Y.; Zheng, X.; Yang, J.; Yang, L. *Spectrochim. Acta A* **2009**, *74*, 336. (b) Zhou, Y.; Lu, Q.; Liu, C.; She, S.; Wang, L. *Anal. Chim. Acta* **2005**, *552*, 152.
 13. (a) Fayed, T. A.; Ali, S. S. *Spectrosc. Lett.* **2003**, *36*, 375. (b) Hancock, J. M.; Jenekhe, S. A. *Macromolecules* **2008**, *41*, 6864. (c) Schneiner, S.; Kar, T. *J. Phys. Chem. B* **2002**, *106*, 534.
 14. Tanabe, K.; Suzui, Y.; Hasegawa, M.; Kato, T. *J. Am. Chem. Soc.* **2012**, *134*, 5652.
-